Journal of Visualized Experiments

Cortical source analysis of high-density EEG recordings in children

--Manuscript Draft--

Manuscript Number:	JoVE51705R4
Full Title:	Cortical source analysis of high-density EEG recordings in children
Article Type:	Invited Methods Article - JoVE Produced Video
Keywords:	EEG, electroencephalogram, development, source analysis, paediatric, minimum-norm estimation, cognitive neuroscience, event-related potentials
Manuscript Classifications:	1.8.186.211: Brain; 5.1.370.376.300: Electroencephalography (EEG); 6.1.525.200: Child Development; 6.2.463.188: Cognition; 7.11.561.270: Evoked Potentials
Corresponding Author:	Johannes Michael Christian Bathelt, M.Sc. University College London (UCL) London, UNITED KINGDOM
Corresponding Author Secondary Information:	
Corresponding Author E-Mail:	johannes.bathelt.10@ucl.ac.uk
Corresponding Author's Institution:	University College London (UCL)
Corresponding Author's Secondary Institution:	
First Author:	Johannes Michael Christian Bathelt, M.Sc.
First Author Secondary Information:	
Other Authors:	Helen O'Reilly, Ph.D.
	Michelle de Haan, Ph.D.
Order of Authors Secondary Information:	
Abstract:	EEG is traditionally described as a neuroimaging technique with high temporal and low spatial resolution. Recent advances in biophysical modelling and signal processing make it possible to exploit information from other imaging modalities like MRI that provide high spatial resolution to overcome this constraint 1. This is especially useful for investigations that require the high temporal resolution. In addition, due to the easy application and low cost of EEG recordings, EEG is often the method of choice when working with populations that do not tolerate functional MRI scans well, like paediatric populations. However, in order to use spatial information from structural MRI scans, most EEG analysis packages work with standard head models that are based on adult anatomy. The accuracy of these models is limited 2, because the composition and spatial configuration of head tissues changes dramatically over development 3. In the present paper, we provide an overview of our recent work in utilising head models based on MRI to reconstruct the cortical generators of high-density EEG. We describe how we acquire, process and analyse EEG recordings with paediatric populations in our laboratory, including laboratory setup, task design, EEG preprocessing, MRI processing and EEG channel-level and source analysis.
Author Comments:	
Additional Information:	
Question	**Response**

Justin Cherny, Ph.D.
Science Editor
Journal of Visualized Experiments
1 Alewife Center, Suite 200
Cambridge, MA 02140

Developmental Cognitive Neuroscience Unit
& Biophysics and NeuroImaging Unit
Institute of Child Health
University College London (UCL)
30 Guilford Street
London WC1N 1EH

Friday, 17 January 2014

Dear Dr. Cherny,

Thank you for considering our manuscript "Cortical source analysis of high-density EEG recordings in children" for publication in JoVE. We appreciate the time taken you yourself and the reviewers in evaluating our manuscript and providing constructive criticism.

We have responded in detail to all points raised by the reviewers in the attached document "Response to reviewers' comments" ,and we include a revised version of the manuscript incorporating these changes.

We feel the manuscript has greatly benefited from the review process, and thank you for your time and effort!

Yours

Joe Bathelt

on behalf of all co-authors

Included materials

Title	Version	Date
JoVE1705_R5.docx	4	17/1/14
JoVE Rebuttal 3 - Response to Reviewers' comments	3	17/1/14
Folder of revised figures	4	17/1/14

Mr. Joe Bathelt, MSc
Developmental Cognitive Neuroscience Unit
UCL Institute of Child Health
30 Guilford Street
WC1N 1EH London
+44 (0) 20 7905 2749
johannes.bathelt.10@ucl.ac.uk

Cortical source analysis of high-density EEG recordings in children

Authors:
Mr. Joe Bathelt, M.Sc.
First Author/Corresponding Author
Affiliations: UCL Institute of Child Health
Address: Developmental Cognitive Neuroscience Unit
UCL Institute of Child Health
30 Guilford Street
London WC1N 1EH
United Kingdom
E-mail: johannes.bathelt.10@ucl.ac.uk

Dr. Helen O'Reilly, Ph.D.
Second Author
Affiliations: UCL Institute for Women's Health
Address: Academic Division of Neonatology
Institute for Women's Health
University College London
74 Huntley Street
London WC1E 6AU
E-mail: h.o'reilly@ucl.ac.uk

Dr. Michelle de Haan, Ph.D.
Third Author/Senior Author
Affiliations: UCL Institute of Child Health
Address: Developmental Cognitive Neuroscience Unit
UCL Institute of Child Health
30 Guilford Street
London WC1N 1EH
United Kingdom
E-mail: m.de-haan@ucl.ac.uk

Keywords
EEG, electroencephalogram, development, source analysis, pediatric, minimum-norm estimation, cognitive neuroscience, event-related potentials

Short Abstract
In recent years, there has been increasing interest in estimating the cortical sources of scalp-measured electrical activity for cognitive neuroscience experiments. This article describes how high-density EEG is acquired and how recordings are processed for cortical source estimation in children from the age of 2 years at the London Baby Lab.

Long Abstract
EEG is traditionally described as a neuroimaging technique with high temporal and low spatial resolution. Recent advances in biophysical modelling and signal processing make it possible to exploit information from other imaging modalities like structural MRI that provide high spatial resolution to overcome this constraint [1]. This is especially useful for investigations that require high resolution in the temporal as well as spatial domain. In addition, due to the easy application and low cost of EEG recordings, EEG is often the

method of choice when working with populations, such as young children, that do not tolerate functional MRI scans well. However, in order to investigate which neural substrates are involved, anatomical information from structural MRI is still needed. Most EEG analysis packages work with standard head models that are based on adult anatomy. The accuracy of these models when used for children is limited [2], because the composition and spatial configuration of head tissues changes dramatically over development [3].

In the present paper, we provide an overview of our recent work in utilising head models based on individual structural MRI scans or age-specific head models to reconstruct the cortical generators of high-density EEG. This article describes how EEG recordings are acquired, processed and analysed with paediatric populations at the London Baby Lab, including laboratory setup, task design, EEG preprocessing, MRI processing and EEG channel-level and source analysis.

Introduction

President Barack Obama described the human brain as the next frontier of scientific discovery with high importance for health and economy (http://www.whitehouse.gov/share/brain-initiative). However, like any other field in the natural sciences, neuroscience depends on advances in methodologies and analysis techniques for progress. Two commonly used non-invasive tools in studies about brain function in humans are magnetic resonance imaging (MRI) and electroencephalography (EEG).These tools exploit different physical properties and provide different insights into brain function with unique advantages and disadvantages. MRI uses the magnetic properties of water molecules within magnetic fields to obtain images of living tissues. The subject needs to be placed in a magnet with high field strength. The participant's movement is restricted during this procedure and the participant has to tolerate noise caused by rapid changes in the magnetic field. In addition to structural images, MRI also provides the possibility to measure changes in blood oxygenation to investigate brain function (fMRI). In summary, MRI offers relatively high spatial resolution of up to $0.5mm^3$ with modern high-fields scanners and optimized parameters [4]. In contrast, the temporal resolution of fMRI is limited to the slow kinetics of the BOLD response, which only indirectly reflects the high temporal dynamics of neural activity [5,6].

On the other hand, EEG measures changes in electrical activity caused by the activity of neurons through electrodes placed on the scalp. Recent advances in EEG technology allow quick and easy application of the sensors for short-term or long-term and stationary as well as ambulatory recordings. Because EEG is less restrictive, it is also the method of choice for certain participant populations that do not tolerate the MRI environment well like pediatric and certain geriatric and psychiatric populations. The properties of EEG show an inverse pattern to those of MRI: the temporal resolution is very high with millisecond precision, but the spatial resolution is limited. Electrical currents pass through different tissues between their generator and the EEG electrodes on the surface of the scalp. This leads to mixing and spatial smearing of source activity known as the volume conduction effect. Therefore, activity measured by the electrodes on the surface of the scalp reflects activity from multiple sources that might be distant to the position of the electrode on the head [1.7].

Much work in recent years has been dedicated to the merging of MRI and EEG in order to take advantage of their respective strengths. One line of work is dedicated to the simultaneous acquisition of EEG and MRI in functional studies. Another approach is to use the spatial information provided by structural MRI to take account of the volume conduction

effect through biophysical modelling. The use of structural information for source reconstruction of EEG recordings is particularly useful for studies involving a pediatric population. The investigation of the development of brain function is central to understanding how complex cognitive skills are built on top of simple precursors [8].

These investigations help to highlight changes in the neural substrates and response properties that correlate with changes in behavioral performance. However, the investigation of brain function and cognition during development also poses specific challenges. Particularly, the opportunity for functional MRI studies is limited as young children and infants either have to be asleep or sedated to obtain MRI data without movement artefacts and negative impact on participant wellbeing. Further, EEG is perceived as less risky and invasive by parents, which makes the recruitment of research participants easier. Therefore, EEG is the method of choice for many investigations of brain function in young children. Methodological advances in EEG systems allow the application of high-density electrode arrays with 128 or more channels within minutes. Ease of application and wearing comfort are sufficient to even allow EEG recording in the youngest infants. However, often researchers are not only interested in the temporal dynamics of responses to particular stimuli, but would also like to compare the neural substrates that mediate the responses.

A prevailing assumption in channel-level ERP analysis comparing different age groups is that the same neural substrates respond, but that the timing or response amplitude varies across ages [9]. Similar scalp topography is often used as an indicator of similar underlying neural activity. However, many different source configurations can lead to similar scalp topographies [10]. By applying source estimation, this uncertainty can be reduced and quantified. The independence of observations is critical for network accounts of brain function: If the sources are mixed, correlations will be biased towards higher local connectivity. Source reconstruction can be applied to reduce this bias[11]. Alternatively, differences in timing and phase can be used for connectivity analysis, but these mathematical models require assumptions that are hard to evaluate in non-simulated data [12]. In summary, source estimation provides additional information to channel-level EEG and ERP analysis based on knowledge about anatomy and biophysical properties of tissue.

Different algorithms have been devised to find solutions to the inverse problem. These algorithms fall broadly into two categories: parametric and non-parametric [13]. Parametric models assume one or multiple dipoles that may vary in location, orientation and strength. In contrast, non-parametric models contain a large number of dipoles with fixed location and orientation. In these models, the scalp electrical activity is explained as a combination of activations in the fixed dipoles [10,13,14]. Non-parametric, distributed source models can be based on knowledge about anatomy and conductivity in different media. Boundary Element Models incorporate conductivity values for the main tissues of the head with different shells for the brain, cerebro-spinal fluid, and skull. This is based on the assumption that conductivity is mostly constant within each compartment, but that marked changes occur at the boundary of different compartments. Finite element models are based on further segmentation of MR scans into grey and white matter so that conductivity values can be assigned to each voxel [15].

In practical terms, non-parametric models are particularly useful for source reconstruction in complex cognitive tasks, in which the number of areas involved may not be known [10]. Boundary element models are most widely used in the current literature, probably because the more accurate Finite Element Models pose comparably high computational demands.

Further, there is considerable inter-individual variability in grey and white matter so that FEMs should be based on individual MRI scans.

Non-parametric models require a second step for matching the scalp-measured activity to the predictions of the forward model. Again, different approaches with different advantages and drawbacks have been discussed in the literature (see Michel et al. 2004 for an overview). The most widely used algorithms are based on minimum-norm estimation (MNE), which matches the scalp-measured activity to a current distribution in the forward model with the lowest overall intensity [16]. MNE is biased towards weak and superficial sources. Depth-weighted MNE algorithms try to reduce the surface bias by introducing weighting matrices based on mathematical assumptions [10]. The widely used LORETA approach is also based on weighted MNE, but additionally minimizes the Laplacian of sources, which leads to smoother solutions [17,18]. LORETA has been found to perform best for single sources in simulation studies [19,20]. However, LORETA may lead to over-smoothing of solutions. Depth-weighted MNE is preferable when the sources are unknown or multiple sources are likely to be present [13 16]. Comparing the results of different algorithms to evaluate the influence of different model assumptions is recommended.

In summary, source reconstruction through modelling methods has been limited for children until recently. This is because most EEG analysis software relies on head models based on adult anatomy that substantially limits the accuracy of source solutions in children [2,8]. The cheap access to computational power and the provision of user-friendly software for source reconstruction make it possible to overcome these limitations. Applying source estimation to the EEG provides two important advantages over analysis based on channel-level observations alone: improved spatial resolution and independence of observations.

Source estimation may not be informative in some cases: Good coverage of the head is required to distinguish sources. High-density systems with 128 or more electrodes are recommended [10,15]; a sparser coverage will act as a spatial filter leading to more wide spread source activation or false-negative results [10]. Furthermore, source reconstruction based on the method described in this article has only been reported for cortical generators. Therefore, it is less suitable for testing hypotheses about subcortical substrates or cortical-subcortical interactions. Lastly, source analysis should be based on detailed prior hypotheses about the cortical substrates, taking the existing literature from other imaging modalities into account. Spatial filtering techniques may also be used to improve the spatial resolution of the EEG signal by reducing spatial mixing on the scalp level. Alternative methods to reduce the influence of volume conduction effects without head modelling are used, e.g. Laplacian filtering [21] or Current Source Density analysis [22]. However, these methods do not provide more information about neural generators as volume conduction effects are not only restricted to sensors in close spatial proximity [1].

In the following sections, the article describes how experiments for the investigation of brain and cognitive function in children from 2 years of age are designed at the London Baby Lab. Next, EEG data acquisition with high-density low-impedance systems with children is discussed. Then, EEG preprocessing and analysis on the channel level is presented. Lastly, the article focuses on the processing of structural MRI data for cortical source reconstruction and analysis of source level signals.

Protocol

1. Designing EEG & Event-related potential experiments for children

Note: A simple experiment was designed for the purposes of this article that may be used to investigate face processing in young children. The following section will describe the experiment and explain how to implement it using Matlab R2012b and Psychtoolbox V3.0.11 [23,24]. Pictures taken from the NimStim set of emotional facial expression [25] were used for this example. This stimulus set is available for research purposes upon request (http://www.macbrain.org/resources.htm).

1.1. Transfer the RGB pictures to grey scale to reduce differences between stimuli. See Table 1. Note: These commands require the Image Processing Toolbox (http://www.mathworks.co.uk/products/image/). Free alternatives may be found through the File Exchange (https://www.mathworks.co.uk/matlabcentral/fileexchange).

1.2. Use experimental control software to implement the experiment with precise timing for stimulus presentation triggers using a series of commands (see Table 1 for an example).

2. Data Acquisition

2.1.Ensure that the child is comfortable with the testing environment. Allow younger children to sit on the lap of their caregiver or in a comfortable child's seat. Let the child see and feel the sensor net before applying it to the child's head. If there is an extra net, have the parent also tries one on, or place one on a doll or stuffed teddy.

2.2.Measure the maximum head circumference to select the correct net size for the child. Use a measuring tape and hold it to the nasion. Then measure around the head around the maximum circumference (~1cm above the inion). Note: Keep a record of the measured head circumference and the sensor net used for later analysis[26]. It helps if the parents head is also measured to make children more comfortable with the situation.

2.3. Identify the vertex of the head at the intersection of the mid distance between nasion and inion and left and right periauricular point. Mark this point with a china pen to ensure that the vertex channel is correctly positioned when applying the net.

2.4. Apply the sensor net and make sure that key channels are aligned with the anatomical landmarks (nasion, inion, vertex and left/right mastoids). Note: For the most accurate results, the position of the channels on the head can be digitally acquired using special digitization equipment. Researchers wishing to acquire the sensor position should refer to the appropriate hardware and software manuals. Alternatively, electrode maps that assume standard placement of electrodes along anatomical landmarks can be used. These maps can be warped to age-appropriate head models as described in the analysis section.

2.5. Ensure that channels have good contact with the scalp by positioning the sensors individually; gently twist each sensor from side to side to move hair out of the way.

2.6. Measure channel gains and channel impedances. Click "Start" to begin the recording in NetStation EEG recording software and start gain and impedance measurement. If

measurement does not automatically start, use the “Calibrate Amplifier” and the “Measure Net Impedances” button.

2.7. Check the recording software for channels with impedances higher than 50kΩ which will appear red. Apply additional electrolyte solution with a pipette to lower channel impedances. Check the EEG display for channels that show high frequency activity despite low impedance or noticeably less activity than surrounding channels (flat line channels). These channels may have loose contact with the scalp and require adjustment.

2.8. In order to keep children comfortable during the EEG preparation, allow the child to listen to music, watch an age-appropriate cartoon or distract them using another experimenter, e.g. blowing soap bubbles for toddlers.

3. Analysis

3.1. Preprocessing

3.1.1. Digitally filter the data with a high-pass filter with a cut-off at 0.1Hz to remove channel drifts [27] (Table 1).

3.1.2 For ERP analysis, apply a low-pass filter with a cut-off at 30Hz [27] (Table 1).

3.1.3 Epoch the continuous data according to the trigger codes set during recording. For most experiments, use a baseline of 200ms prior to stimulus onset and a post-stimulus interval of 600ms to cover the time interval of interest (Table 1).

3.1.4 Remove epochs that contain movement or blink artefacts: mark channels with a peak-to-peak amplitude higher than 150mV - adjust this threshold depending on the participant group and data quality. For consistency, use the same threshold for all participants in one study. If a channel is above this threshold in more than 30% of the epochs, remove the channel (channel activity may be interpolated from surrounding channels, if these contain acceptable data). If more than 20% of the channels are marked as bad in an epoch, remove the epoch. If more than 20% of channels are rejected by the algorithm or less than 50% of epochs are retained, consider removing the dataset from further analysis (Table 1).

Note: The percentage thresholds for epoch and channel rejection are ballpark figures that remove a sufficient amount of noise in our experience. The amount of artefact in the recording is likely to be different using other participant groups, experimental paradigms or EEG systems. The experimenters may want to adjust the percentage thresholds and check if they are satisfied with the artefact rejection. Alternatively, experimenters can reject trials that contain artefact through visual inspection.

3.1.5 Re-reference to average reference by subtracting the mean activity across channels from each channel (Table 1). Note: The vertex electrode is typically used as the recording reference in NetStation.

3.2 Artefact correction using Independent Component Analysis:

3.2.1 Import the data into the FASTER toolbox [28] and run the automatic artefact rejection algorithm on the data (Table 1).

3.2.2 Use the Graphical User Interface (GUI) for FASTER; to open the GUI, type FASTER_GUI into the command line.

3.2.3 Deselect the filtering options in the filtering menu as the data has already been filtered before the epoching.

3.2.4 Specify the number of channels: 126 EEG channels with 2 electrooculagram (EOG) channels.

3.2.5 Enter the markers used for epoching the data as strings in a cell array. For the presented case enter: {'face','scra'} for the face and scrambled face conditions.

3.2.6 Select the channels for the independent component analysis (ICA). Typically select all recording channels, incl. external non-EEG channels.

3.2.7 Specify the input and output folder in the right pane of the GUI.

3.2.8 Select the appropriate channel file for the recordings. Note: channel files for most EEG system can either be downloaded from the manufacturer or can be downloaded from the EEGLAB website.

3.2.9 Click RUN to start FASTER processing. Depending on the length of the recordings and the number of files, this processing can take several hours.

3.2.10 Visually inspect the recordings, independent component maps and ERPs after the processing.

3.3 Channel-level analysis of event-related potentials data

3.3.1 Combine several channels to form a virtual channel with better signal to noise ratio (Table 1). Note: The selection of channels should be based on previous reports in the literature or *a priori* hypotheses. Selecting channels that show the highest amplitude within a given time window is not advised [29].

3.3.2 Obtain measures like peak amplitude, mean amplitude and peak latency to characterize the waveform and perform statistical tests (Table 1).

3.4 Create Boundary Element Models (BEM)

3.4.1 Segment the anatomical MRI scan with FreeSurfer. Note: For the most accurate results, base the boundary element model on individual MRI scans for each participant. If this is not feasible, average MRI templates that match the participants' age as closely as possible should be used. Please note that BEMs cannot be used for children under 24 months. Boundary element models assume that each shell (brain, skull, skin) consists of a closed shell. However, in young children the fontanelles in the skull are not closed, which violates the closed shell assumption.

3.4.1.1 In order to install FreeSurfer software, first download it from the FreeSurfer website (http://freesurfer.net/fswiki/DownloadAndInstall). Next, set up the shell environment include FreeSurfer; for .bashrc, include the following commands in the .bashrc file:

3.4.1.1.1 Export FREESURFER_HOME=/Applications/freesurfer/

3.4.1.1.2 Source $FREESURFER_HOME/FreeSurferEnv.sh

Note: These commands assume that the FreeSurfer folder is in the Applications folder on a Unix system. There are more details on how to setup FreeSurfer with alternative shell environments, e.g. csh/tcsh, or operating systems on the FreeSurfer website (http://freesurfer.net/fswiki/DownloadAndInstall).

3.4.1.2 Next, define the Subject directory, i.e. the folder that the output will be written to using the following command:

3.4.1.2.1 export SUBJECTS_DIR=/…/BEMs/
Note: The results may be written to any folder on the system.

3.4.1.3 Next, change the working directory to the folder that contains the MRI file for the Boundary Element Model using the following command:

3.4.1.3.1 cd /Users/joebathelt/Neurodevelopmental_MRI_database/Children/Brain/
Note: Any folder on the system may be specified using the syntax of the cd command. This is an example of the primary researchers file structure.

3.4.1.4 Finally, start the reconstruction using the following commands:

3.4.1.4.1 recon-all -i <mri_file> -subjid <subject_id>

3.4.1.4.2 recon-all -all -subjid <subject_id>
Note: <mri_file> needs to be replaced with the filename of the desired MRI scans in the current directory. <subject_id> can be replaced with any name. FreeSurfer will create a folder with this name in the subject directory. Depending on the system used, the last commands may require some time to run.

3.4.2 Check the FreeSurfer segmentation for incorrect segmentation, e.g. overlapping spheres, anatomically unlikely compartments etc. by importing the segments into BrainStorm and use the display tools in the GUI:

3.4.2.1 In BrainStorm, select the anatomy pane. Import the segmented MRI by right-clicking on the subject and selecting “Import Anatomy Folder”. Ensure the folder with the FreeSurfer output is selected. Inspect the segmentation visually by right-clicking and selecting “Display”. Note: Alternatively, FreeSurfer commands can be used. A detailed description can be found on the FreeSurfer website: http://surfer.nmr.mgh.harvard.edu/fswiki/RecommendedReconstruction. If region of interest analysis based on anatomical parcellation is desired, the FreeSurfer functions mris_ca_label, mri_annotation2label and mri_mergelabels can be used. Refer to the FreeSurfer publications and online help pages for more detailed information.

3.5 Estimate the source activity in BrainStorm

3.5.1 Start BrainStorm by typing "brainstorm" in the command window.

3.5.2 Create a new protocol by selecting New Protocol from the File menu.

3.5.3 Add a new subject to the protocol by selecting New Subject from the File menu.

3.5.4 Import EEG data for the participant by right-clicking on the subject and selecting "Import MEG/EEG".

3.5.5 Import a channel file by right-clicking and choosing "Import channel file". Note: The channel file needs to be aligned to the MRI for source reconstruction. BrainStorm uses a system of 4 anatomical reference points that the user needs to mark in the MRI. Please refer to the BrainStorm tutorials for more information (http://neuroimage.usc.edu/brainstorm/CoordinateSystems). The standard position as defined by a channel file for a certain EEG system or, ideally, the head positions that were digitised prior to the EEG recording can be used.

3.5.6 Check that the BEM and the channels align as expected: Right-click on the channel file for the subject and navigate to "MRI registration" and "Check". Note: If the spheres within the model are overlapping or if the channels are within the BEM, the source reconstruction will produce incorrect results. Adjust the alignment by using the "Edit" option in the "MRI segmentation" menu.

3.5.7 Calculate the noise covariance matrix from the baseline of each epoch by right-clicking on the participant and choosing "Noise Covariance Matrix" and "Calculate from Recording". Note: The authors of the BrainStorm toolbox recommend using a diagonal noise covariance matrix for short recordings (~ less time points than channels) and a full one for longer recordings. Please refer to the BrainStorm Source Estimation tutorial for more information: http://neuroimage.usc.edu/brainstorm/Tutorials/TutSourceEstimation .

3.5.8 Calculate the Source Model by right-clicking on the subject and selecting "Compute source model".

3.5.9 Calculate the inverse solution using depth-weighted Minimum-Norm Estimation by right-clicking on the subject and selecting "Compute Source" and "Minimum-norm estimation". Note: Other options (dSPM, sLORETA) are available. Each option has different advantages and drawbacks. The algorithm should be selected based on *a priori* considerations and previous reports in the literature. Further, some algorithms are better in resolving focal activation in certain areas, whereas others are more suitable for wide-spread activation. MNE was used for this study based on previous reports in the literature [16]. For consistency, the same algorithm for inverse solution should be used for all participants in one study. Researchers may also want to compare how robust findings are to the application of different inverse solution algorithms.

3.5.10 Repeat Section 3 for all participants in the study. Note: Either use the graphical batching interface or scripts to repeat processing steps for participants. See the BrainStorm documentation for instructions (http://neuroimage.usc.edu/brainstorm/Tutorials/TutRawScript).

3.5.11 Average source activity over trials per participants by dragging the recordings to the Process Menu and selecting “Average” and “By condition (subject average)”.

3.5.12 Contrast the condition by selecting the “Processes 2” and dragging each condition in one window. Then, select “Test” and “Student’s t-test” or “Student’s t-test (paired)” depending on design. To perform multiple comparisons, set amplitude and area thresholds in the display of the resulting statistical map in the “Stat” menu. Note: Alternatively, the activation maps can be exported to SPM (http://www.fil.ion.ucl.ac.uk/spm/) for more in-depth statistical analysis (http://neuroimage.usc.edu/brainstorm/ExportSpm12).

3.5.13 Calculate the event-related response for a region of interest. For parcellation-based ROIs, load the FreeSurfer parcellation by right-clicking on the cortex surface in the anatomy menu and select “Import labels”. Navigate the corresponding file and load it. Now, select a ROI in the “Scout” pane of the functional data menu.

3.5.14 Obtain the ROI event-related activity by dragging files to the Process 1 window and select “Extract Scout Time Series” from the Sources menu. Note: several ROIs can be selected simultaneously and the ROI time series can be exported for further plotting and analysis by right-clicking on the scout time series data and selecting “Export to Matlab”.

Representative Results

Designing ERP experiments for infants and children is often challenging, because of their limited capacity to tolerate long repetitive experiments [30]. This problem is further aggravated when the experimenter plans to apply source reconstruction, because accurate source reconstruction will require a high signal to noise ratio [1]. Figure 1 displays an experimental protocol for the investigation of face processing mechanisms that can be used with very young children. The paradigm is adapted to a) minimize eye blinks and eye movements during stimulus presentation, because children will be less able to control eye movements than adult volunteers b) make the experiment more engaging by adding attention grabbers after the inter-stimulus interval. Eye blinks and eye movements are controlled by presenting a fixation cross shortly before the stimulus in order to draw attention to the center of the screen. Further, the stimulus duration is set to 500ms, which allows conscious perception of the stimulus while minimizing the time for scanning the image with eye movements. The attention grabber consists of a child-friendly image presented with a simultaneous sound. A random selection of different attention grabber stimuli can be used to keep the task interesting for the child. The next trial can be started by the experimenter, when it is clear from the monitoring system that the child is looking at the center of the screen again. In addition, stories can be used to help older children attend to the screen. It is often helpful to practice tasks with children before the EEG recording to make sure that the child understands the task. Screening questions or scores obtained in the practice session can be used as covariates in later analyses.

When calculating the number of repetitions needed for the experiment, it is important to take into account that many trials may be lost due to inattention or movement artefact when working with children. As a rule of thumb, the necessary number of repetitions should be doubled compared to adult studies. The attention span and cooperation is limited in children compared to adults. Therefore, take the specific needs of children in mind when designing the task. A long task can be broken into several blocks of shorter tasks with breaks in between.

Typically, the number of conditions that can be included in the experiment is smaller for very young children, as they will not be able to cooperate for the longer periods needed to obtain sufficient trials for many stimulus conditions.

The figures presented are based on a recording with a 6 year old boy (6 years 3 months). The head model was based on an average MRI template of 6 year olds [31]. Figure 5 shows channel-level event-related potential responses (ERP) to face and scrambled face stimuli. The waveform of the ERP over posterior channels shows the expected pattern of a positive deflection with a peak around 100ms followed by a negative deflection with a peak around 180ms and a subsequent broad positive deflection. Based on the topography, time course and nature of the paradigm, these deflections are likely to represent the P100, N1 and late positive potential component. Further, the early negative deflection is significantly larger for face stimuli compared to scrambled faces. Therefore, it is likely to reflect the face specific N170 component. The topographic maps in Figure 5 show the voltage distribution between 250 and 300ms. Negative voltage with a maximum over right occipito-temporal channels in the faces condition is evident.

Figure 6 shows the statistical comparison of source activity projected based on a standard adult head model and an age appropriate head model. Source reconstruction was based on a boundary element model (BEM) with depth-weighted minimum-norm estimation (wMNE) and full noise covariance matrix in Brainstorm v. 3.1 [32]. The default MNI Colin27 BEM was used as the adult model. Source activity was averaged over time between 250 and 300ms in line with face-specific responses on the channel level.

The map shows the results of a Student t-test comparison between the faces and scrambled faces condition corrected for multiple comparisons using false discovery rate (FDR). The results show significantly stronger source activation over the temporal lobe in the faces compared to the scrambled faces condition. The localization using the age-appropriate model is more focal with strong differences on the ventral surface of the temporal cortex. Localization based on the adult-head model is more disperse and shows source activity differences on the right medial and superior temporal gyrus that is mostly absent on the map based on the age appropriate head model.

Figure 6 shows the source level ERP for the right fusiform gyrus. A negative deflection about 190ms after stimulus onset can be identified in the response to faces, but not to scrambled faces. Based on this, one can conclude that fusiform activity contributes to the N170 response in the faces condition, but not to the N1 response in the scrambled faces condition.

Figure Captions

Figure 1: Example of a face perception experiment suitable over a wide age range
The experiment consists of visual presentation of images of faces or scrambled faces. The stimuli are physically identical, but the spatial arrangement is randomized in the scrambled condition. Each trial begins with central presentation of a fixation cross to minimize eye movements during stimulus presentation. The duration of the fixation cross presentation is randomized to avoid influences of entrainment over multiple repetitions. The stimulus is presented over a duration of 500ms. The short duration also minimize the chance of eye movements during the presentation window. An attention grabbing stimulus is presented after

an inter-trial interval with random duration between 1 and 2s. The attention grabber is particularly useful for very young participants that are not likely to attend to many trials of non-engaging material in sequence. The experiment can start the next trial, when the participant is looking on the screen in response to the attention grabber.

Figure 2: Flow diagram for the threshold rejection algorithm. The algorithm compares the maximum of each EEG channel in each epoch to a set threshold. If a channel contains maximum activity above the threshold, the channel is marked as bad. If more than 20% of channels are bad in a given epoch, the epoch is rejected. After epoch rejection, the maximum activity in each channel is compared to the threshold again. If a channel contains activity above the threshold in more than 30% of all epochs, the channel is rejected. If more than 20% of channels are rejected by this procedure or less than 50% of epochs per condition are left after epoch rejection, the dataset should be excluded from further analysis.

Figure 3: Automatic artefact correction using the FASTER toolbox[28]**.** The figure shows options that need to be changed to use the FASTER toolbox with the setup and processing pipeline described in this article: 1. Filtering should be disabled, because the dataset has already been filtered 2. The number of channels needs to be adjusted. The EEG system used in this article has 126 channels with 2 EOG channels. 3. Event-markers for time locking need to be specified as a cell array of strings. 4. The time window for the event-related response needs to be supplied. This has to be identical to the window used in the earlier epoching step. 5. The user has to define channels for the independent component analysis (ICA). In most cases, this would comprise all EEG channels and relevant external channels like the eye channels (EOG). 6. The indices of the eye channels also need to be adjusted to the EEG system used. For the EEG system described, these would be channels 125 and 128.

Figure 4: Source analysis in Brainstorm[32]
1. After importing the EEG dataset and FreeSurfer surfaces, the Boundary Element Model (BEM) can be calculated by selecting "Compute head model" in the "Source" menu. 2. The noise covariance matrix can be calculated from the recordings by selecting "Compute noise covariance". If the recording is long enough, i.e. more time points than sensors, the full covariance matrix can be computed, otherwise a diagonal matrix is recommended. 3. After computing the head model and noise covariance matrix, it is possible to obtain the inverse solution. Different algorithms may be used. The depth-weighted Minimum Norm Estimation (wMNE) algorithm was used for this article. 4. The time course of source activity in regions of interest (ROI) can be extracted, by selecting "Extract Scout Time Series" from the "Source" menu. ROIs from automatic cortical parcellation in FreeSurfer were used for this example.

Figure 5: Event-related potentials response (ERP) to face and scrambled face stimuli over right occipito-temporal channels.
The ERP shows a more negative deflection between 130 and 220ms after stimulus onset on the right side for faces compared to scrambled faces. These properties are in line with previous reports about the N170 component [33].

Figure 6: Comparison of source localisation between a default adult head model and an appropriate head model
The top row of the figure shows the MNI adult boundary head model colin27 on the left and an age appropriate head model based on a FreeSurfer parcellation of an average MRI template for 6 year-old children on the right. The locations of co-registered electrode

locations are also presented. The recording was obtained from a 6 year-old boy (6 years 3 months). The second and third row show results of a statistical comparison between activation maps of MNE source reconstruction in the faces compared to the scrambled faces condition based on a t-test corrected for multiple comparison using False Discovery Rate (FDR). The color map illustrates the effect size with red indicating higher activity in the faces condition and blue showing higher activity in the scrambled faces condition. Please note that no amplitude or size thresholds were applied. The localization appears more focal on the ventral surface of the temporal pole using the age-appropriate head model compared to the adult BEM.

Figure 7: Source ERP of the right fusiform gyrus in response to faces and scrambled faces based on source reconstruction of a recording obtained from a 6 year old boy (6 years 3 months) using an age appropriate BEM with MNE

The source ERP show a more negative deflection around 250ms after stimulus onset in the faces condition compared to the scrambled faces condition. This activity is likely to reflect the contribution of the right fusiform gyrus to the N170 component in the faces condition.

Table 1: MATLAB commands to implement the example experiment and analyze high-density EEG recordings on channel- and source-level. The table summarizes the code to implement the faces vs scrambled faces example experiment. Further, the code for pre-processing the raw EEG is presented. In addition, methods for extracting waveform characteristics for channel-level analysis of the event-related response are shown.

Discussion

The present article describes the recording and analysis of high-density EEG for reconstruction of cortical generators using boundary-element models based on age-appropriate average MRI templates and depth-weighted minimum-norm estimation in a standard ERP paradigm suitable for children. In this paradigm, pictures of faces and scrambled faces are presented. Different authors used this paradigm to investigate the development of face processing mechanisms over development [35]. On the channel level, more negative deflections over right occipito-temporal channels are described for the face condition to the scrambled face condition. The topography, latency and response characteristic are consistent with the N170 component [34]. Previous source and simultaneous EEG-fMRI investigations report that the fusiform gyrus is a likely generator of the N170 response. The results of the current analysis show that source inversion with a depth-weighted boundary element model (BEM) can be used to localize source activity in the fusiform gyrus in the face-scrambled face paradigm on the level of individual participants. The use of head models based on the individual participant's anatomy or the use of age-appropriate averaged anatomical scans for developmental studies, in which the individual anatomy is not available, will allow the most accurate source localization [2]. Further, regions of interest can be identified based on anatomical knowledge or automatic parcellation algorithms to investigate the event-related response of particular cortical regions.

There are several limitations to source reconstruction, particularly in developmental samples, at the moment. First, source reconstruction based on average templates for different age groups assumes that the individual shows typical brain development for their chronological age, which might not necessarily be the case, especially in patient groups. For example, various studies described atypical trajectories in brain growth for children born preterm [36] or children with autism [37]. It is hard to estimate how these anatomical differences will influence

the accuracy of the inverse solution and bias results of comparisons between atypical and typical control groups.

Second, forward models such as the boundary element model (BEM) do not incorporate conductivity in-homogeneities within compartments, e.g. differences between grey and white matter. The accuracy for subcortical sources is therefore limited. Source solutions were restricted to subcortical sources for that reason. Finite element models may be applied for more accurate resolution of subcortical generators. With solutions restricted to the cortex, it is important to keep in mind that activation in cortical regions may reflect underlying subcortical causative mechanisms, e.g. feedback communication via thalamic loops. Therefore, causal inferences about the involvement of cortical regions are limited unless more complex models are used that are currently only available for typical adult anatomy, e.g. Dynamic Causal Modelling [38,39].

Further, Boundary-element models assume closed shells for each compartment. However, young infants have soft spots in their skulls, where the sutures between the cranial bones are not fully merged [15]. This violation of BEM assumptions severely limits the applicability of source reconstruction with BEMs in infants younger than 2 years of age. Finite-element models may be used for source reconstruction in this age range.

Third, even though age-appropriate head models were used for source reconstruction, conductivity values based on adult samples were used to model conductivity within each compartment. However, tissue conductivity is likely to change over development, e.g. through increases in bone density [15]. Conductivity values for tissue types used in BEMs for human infants and children are currently not available to our knowledge.

Acknowledgements
We want to thank Prof. John Richards, University of South Carolina, for granting us access to the Developmental MRI database and helpful discussions. We would also like to thank our funders Great Ormond Street Children's Charity, UCL Impact & Grand Challenges.

Disclosures
None of the authors declare conflicting financial interests

References
1. Michel, C. M. & Murray, M. M. Towards the utilization of EEG as a brain imaging tool. *NeuroImage* **61** (2), 371–385, doi:10.1016/j.neuroimage.2011.12.039 (2012).
2. Brodbeck, V., Kuhn, A., *et al.* EEG microstates of wakefulness and NREM sleep. *NeuroImage* **62** (3), 2129–2139, doi:10.1016/j.neuroimage.2012.05.060 (2012).
3. Sanchez, C. E., Richards, J. E. & Almli, C. R. Age-specific MRI templates for pediatric neuroimaging. *Developmental Neuropsychology* **37** (5), 379–399, doi:10.1080/87565641.2012.688900 (2012).
4. Umutlu, L., Ladd, M. E., Forsting, M. & Lauenstein, T. 7 Tesla MR Imaging: Opportunities and Challenges. *RoFo : Fortschritte auf dem Gebiete der Rontgenstrahlen und der Nuklearmedizin*, doi:10.1055/s-0033-1350406 (2013).
5. Logothetis, N. K. Bold claims for optogenetics. *Nature* **468** (7323), E3–E4, doi:10.1038/nature09532 (2010).
6. Logothetis, N. K. What we can do and what we cannot do with fMRI. *Nature* **453**

(7197), 869–878, doi:10.1038/nature06976 (2008).
7. Roche-Labarbe, N., Aarabi, A., *et al.* High-resolution electroencephalography and source localization in neonates. *Human Brain Mapping* **29** (2), 167–176, doi:10.1002/hbm.20376 (2008).
8. Johnson, M. H. Interactive Specialization: A domain-general framework for human functional brain development? *Developmental cognitive neuroscience* **1**, 7–21, doi:10.1016/j.dcn.2010.07.003 (2010).
9. Nelson, C. A. & McCleery, J. P. Use of Event-Related Potentials in the Study of Typical and Atypical Development. *Journal of the American Academy of Child & Adolescent Psychiatry* **47** (11), 1252–1261, doi:10.1097/CHI.0b013e318185a6d8 (2008).
10. Michel, C. M., Murray, M. M., Lantz, G., Gonzalez, S., Spinelli, L. & Grave de Peralta, R. EEG source imaging. *Clinical neurophysiology : official journal of the International Federation of Clinical Neurophysiology* **115** (10), 2195–2222, doi:10.1016/j.clinph.2004.06.001 (2004).
11. Bathelt, J., O'Reilly, H., Clayden, J. D., Cross, J. H. & de Haan, M. Functional brain network organisation of children between 2 and 5years derived from reconstructed activity of cortical sources of high-density EEG recordings. *NeuroImage*, doi:10.1016/j.neuroimage.2013.06.003 (2013).
12. David, O., Cosmelli, D. & Friston, K. J. Evaluation of different measures of functional connectivity using a neural mass model. *NeuroImage* **21** (2), 659–673, doi:10.1016/j.neuroimage.2003.10.006 (2004).
13. Grech, R., Cassar, T., *et al.* Review on solving the inverse problem in EEG source analysis. *Journal of NeuroEngineering and Rehabilitation* **5** (1), 25, doi:10.1186/1743-0003-5-25 (2008).
14. Wendel, K., Väisänen, O., *et al.* EEG/MEG source imaging: methods, challenges, and open issues. *Computational Intelligence and Neuroscience* **2009**, 13, doi:10.1155/2009/656092 (2009).
15. Richards, J. E. Localizing cortical sources of event-related potentials in infants' covert orienting. *Developmental Science* **8** (3), 255–278, doi:10.1111/j.1467-7687.2005.00414.x (2005).
16. Hauk, O. Keep it simple: a case for using classical minimum norm estimation in the analysis of EEG and MEG data. *NeuroImage* **21** (4), 1612–1621, doi:10.1016/j.neuroimage.2003.12.018 (2004).
17. Pascual-Marqui, R. D., Lehmann, D., *et al.* Low resolution brain electromagnetic tomography (LORETA) functional imaging in acute, neuroleptic-naive, first-episode, productive schizophrenia. *Psychiatry Research* **90** (3), 169–179 (1999).
18. Pascual-Marqui, R. D. Standardized low-resolution brain electromagnetic tomography (sLORETA): technical details. *Methods and findings in experimental and clinical pharmacology* **24 Suppl D** (SUPPL. D), 5–12 (2002).
19. Phillips, C., Rugg, M. D. & Friston, K. J. Systematic regularization of linear inverse solutions of the EEG source localization problem. *NeuroImage* **17** (1), 287–301, doi:10.1006/nimg.2002.1175 (2002).
20. Yao, J. & Dewald, J. P. A. Evaluation of different cortical source localization methods using simulated and experimental EEG data. *NeuroImage* **25** (2), 369–382, doi:10.1016/j.neuroimage.2004.11.036 (2005).
21. Tandonnet, C., Burle, B., Hasbroucq, T. & Vidal, F. Spatial enhancement of EEG traces by surface Laplacian estimation: Comparison between local and global methods. *Clinical Neurophysiology* **116** (1), 18–24, doi:10.1016/j.clinph.2004.07.021 (2005).
22. Tenke, C. E. & Kayser, J. Generator localization by current source density (CSD):

implications of volume conduction and field closure at intracranial and scalp resolutions. *Clinical neurophysiology : official journal of the International Federation of Clinical Neurophysiology* **123** (12), 2328–2345, doi:10.1016/j.clinph.2012.06.005 (2012).
23. Brainard, D. H. The psychophysics toolbox. *Spatial vision*, doi:10.1163/156856897X00357 (1997).
24. Kleiner, M., Brainard, D., Pelli, D., Ingling, A. & Murray, R. What's new in Psychtoolbox-3. *Perception* (2007).
25. Tottenham, N., Tanaka, J. W., *et al.* The NimStim set of facial expressions: judgments from untrained research participants. *Psychiatry Research* **168** (3), 242–249, doi:10.1016/j.psychres.2008.05.006 (2009).
26. Chaste, P., Klei, L., *et al.* Adjusting head circumference for covariates in autism: Clinical correlates of a highly heritable continuous trait. *Biological Psychiatry* **74** (8), 576–584, doi:10.1016/j.biopsych.2013.04.018 (2013).
27. Delorme, A., Mullen, T., *et al.* EEGLAB, SIFT, NFT, BCILAB, and ERICA: New tools for advanced EEG processing. *Computational Intelligence and Neuroscience* **2011**, 130714, doi:10.1155/2011/130714 (2011).
28. Nolan, H., Whelan, R. & Reilly, R. B. FASTER: Fully Automated Statistical Thresholding for EEG artifact Rejection. *Journal of Neuroscience Methods* **192** (1), 152–162, doi:10.1016/j.jneumeth.2010.07.015 (2010).
29. Kilner, J. M. Bias in a common EEG and MEG statistical analysis and how to avoid it. *Clinical Neurophysiology*, doi:10.1016/j.clinph.2013.03.024 (2013).
30. DeBoer, T., Scott, L. S. & Nelson, C. A. 12 ERPs in Developmental Populations. *Event-related Potentials: A …* (2005).
31. Sanchez, C. E., Richards, J. E. & Almli, C. R. Neurodevelopmental MRI brain templates for children from 2 weeks to 4 years of age. *Developmental Psychobiology* **54** (1), 77–91, doi:10.1002/dev.20579 (2011).
32. Tadel, F., Baillet, S., Mosher, J. C., Pantazis, D. & Leahy, R. M. Brainstorm: A user-friendly application for MEG/EEG analysis. *Computational Intelligence and Neuroscience* **2011**, 879716, doi:10.1155/2011/879716 (2011).
33. de Haan, M., Johnson, M. H. & Halit, H. Development of face-sensitive event-related potentials during infancy: a review. *International Journal of Psychophysiology* **51** (1), 45–58, doi:10.1016/S0167-8760(03)00152-1 (2003).
34. Earp, B. D. & Everett, J. A. C. Is the N170 face specific? Controversy, context, and theory. *Neuropsychological Trends* **13** (1), 7–26, doi:10.1162/jocn.2007.19.3.543 (2013).
35. Taylor, M. J., McCarthy, G., Saliba, E. & Degiovanni, E. ERP evidence of developmental changes in processing of faces. *Clinical neurophysiology : official journal of the International Federation of Clinical Neurophysiology* **110** (5), 910–915, doi:10.1016/S1388-2457(99)00006-1 (1999).
36. Ment, L. R., Kesler, S., *et al.* Longitudinal brain volume changes in preterm and term control subjects during late childhood and adolescence. *PEDIATRICS* **123** (2), 503–511, doi:10.1542/peds.2008-0025 (2009).
37. Courchesne, E., Townsend, J., *et al.* Impairment in shifting attention in autistic and cerebellar patients. *Behavioral Neuroscience* **108** (5), 848–865 (1994).
38. Litvak, V., Mattout, J., *et al.* EEG and MEG data analysis in SPM8. *Computational Intelligence and Neuroscience* **2011**, 852961, doi:10.1155/2011/852961 (2011).
39. Daunizeau, J., David, O. & Stephan, K. E. Dynamic causal modelling: A critical review of the biophysical and statistical foundations. *NeuroImage* **58** (2), 312–322, doi:10.1016/j.neuroimage.2009.11.062 (2011).

Figure 1 R3

Click here to download Figure: Figure 1 R3.pdf

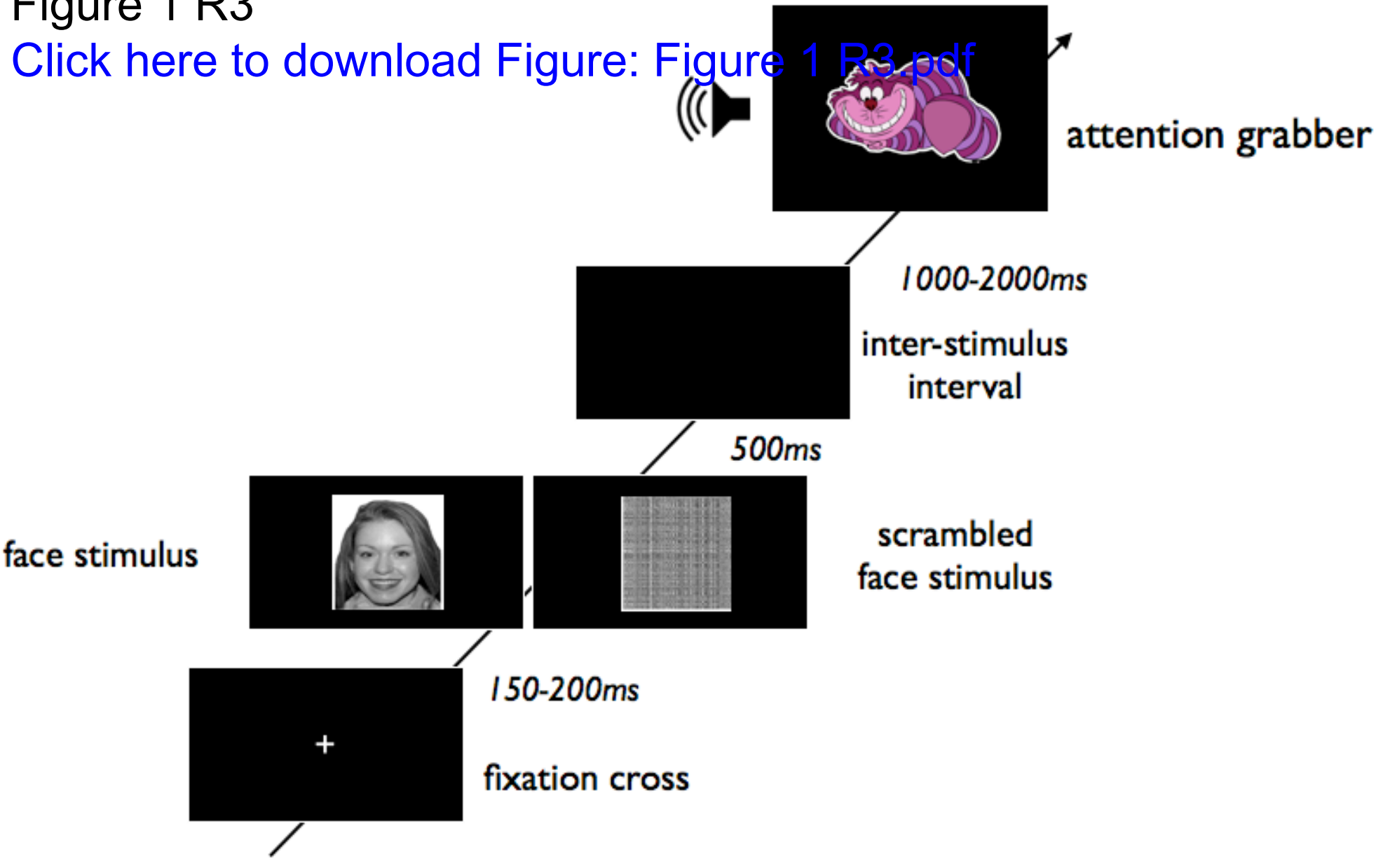

Figure 2 R3
Click here to download high resolution image

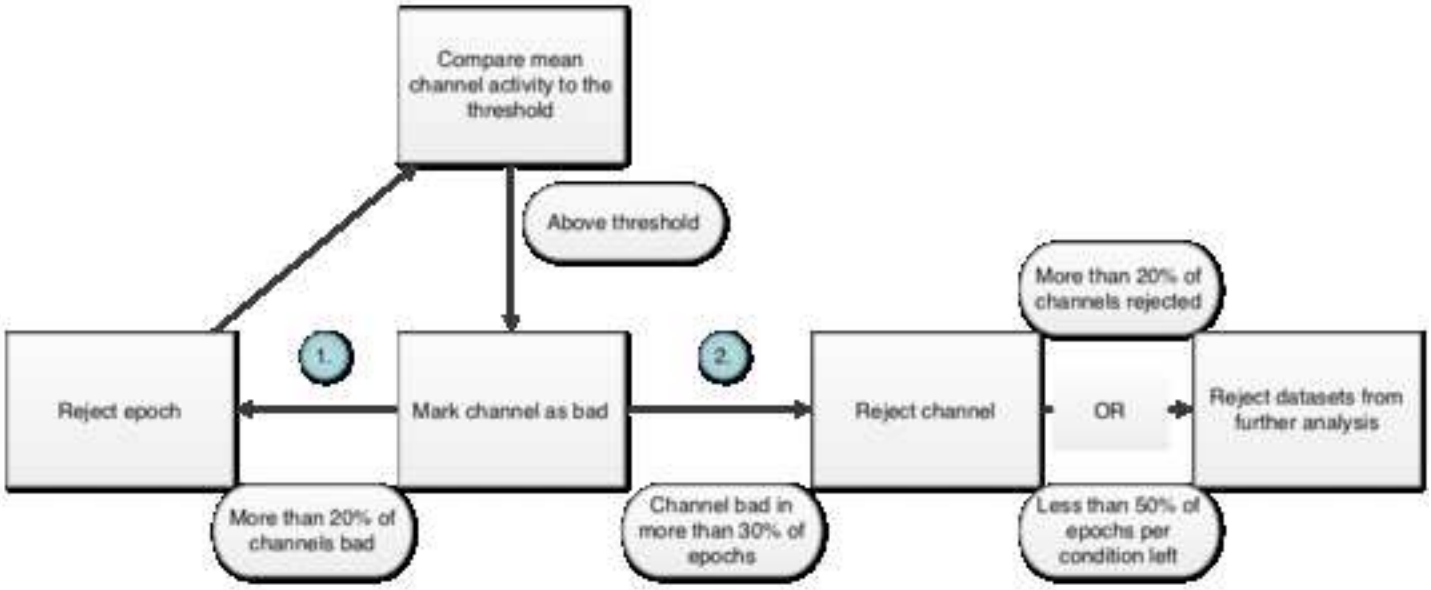

Figure 3 R3

Click here to download high resolution image

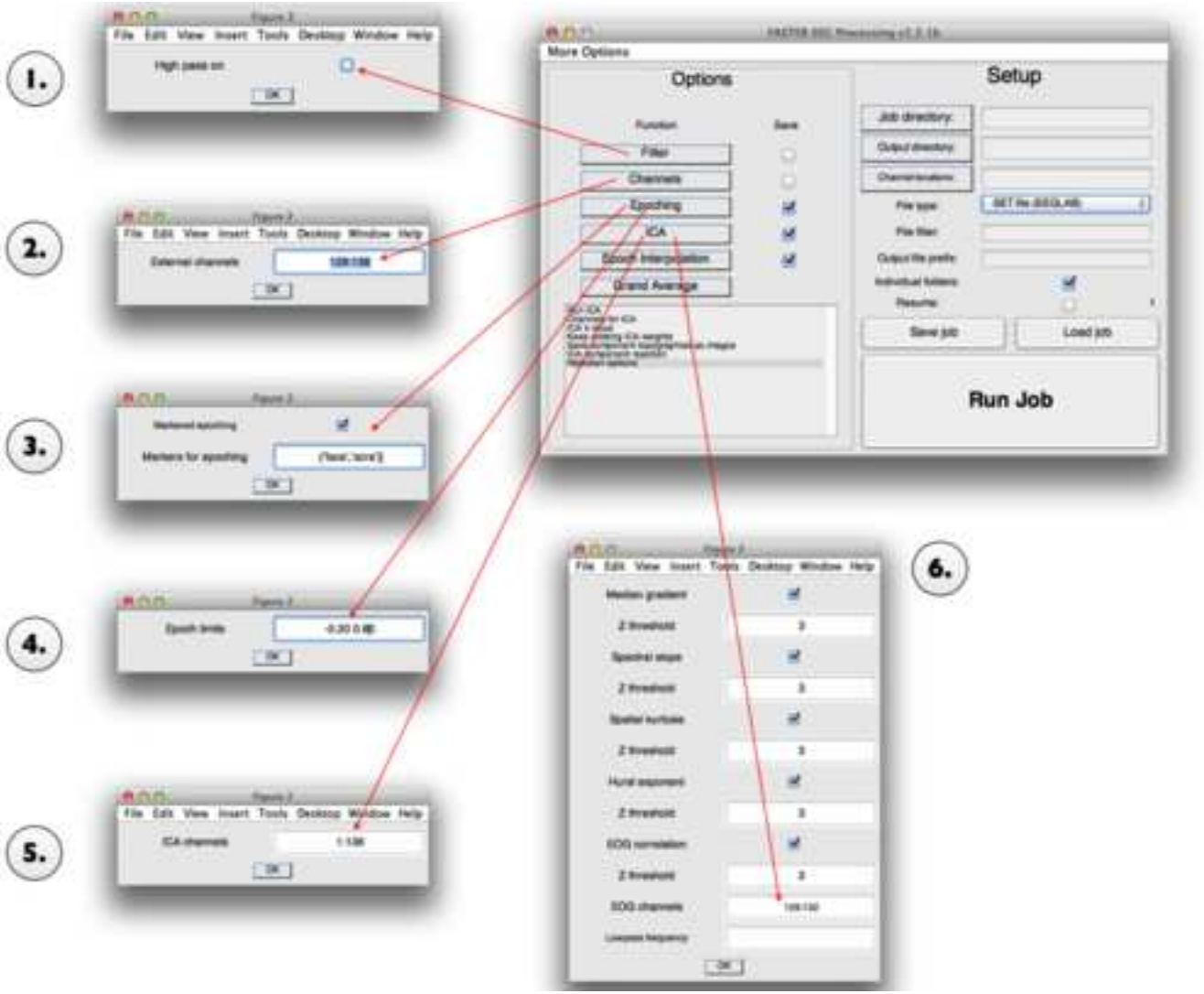

Figure 4 R3

Click here to download high resolution image

Figure 5 R3
Click here to download high resolution image

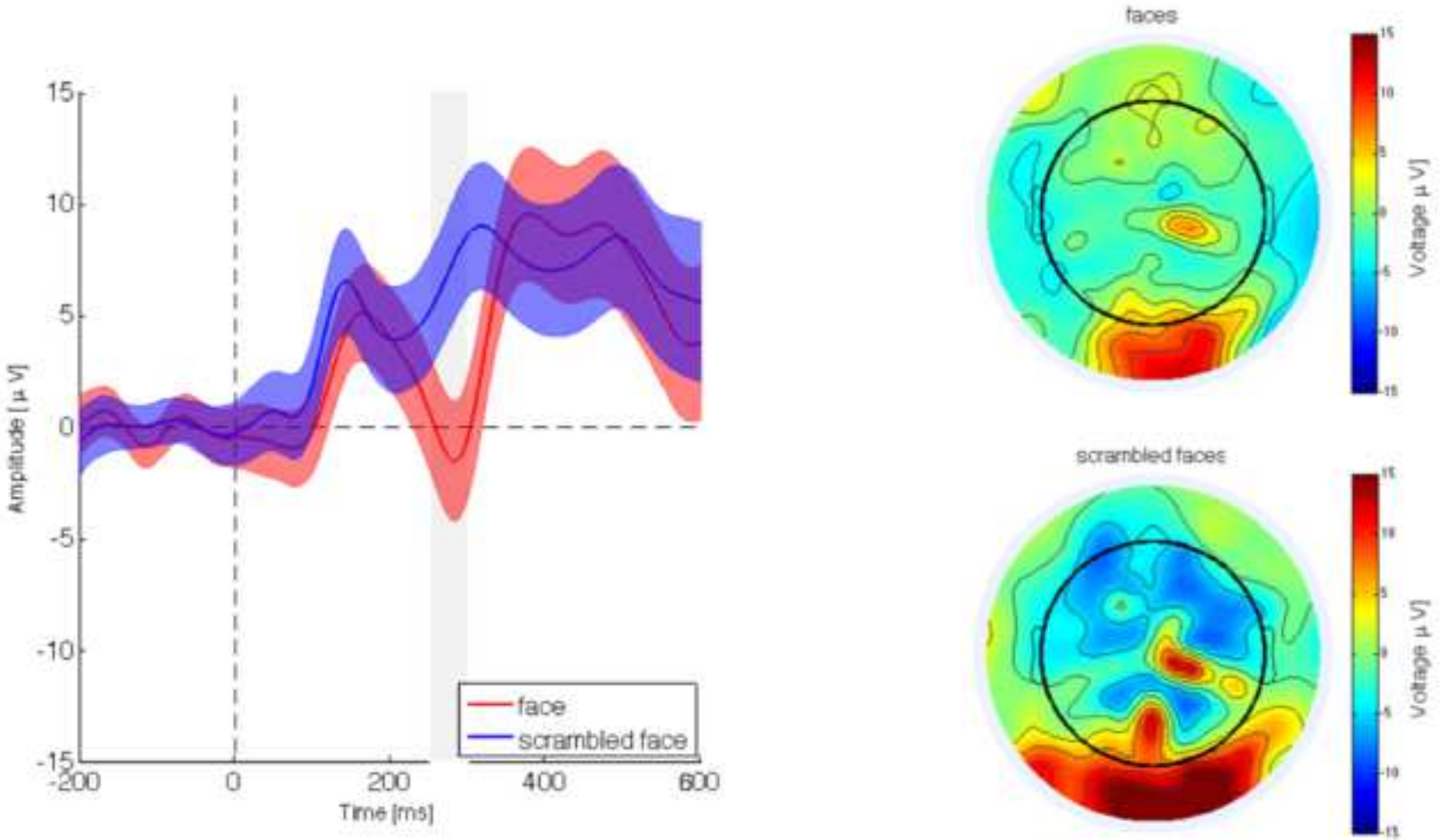

Figure 6 R3

Click here to download high resolution image

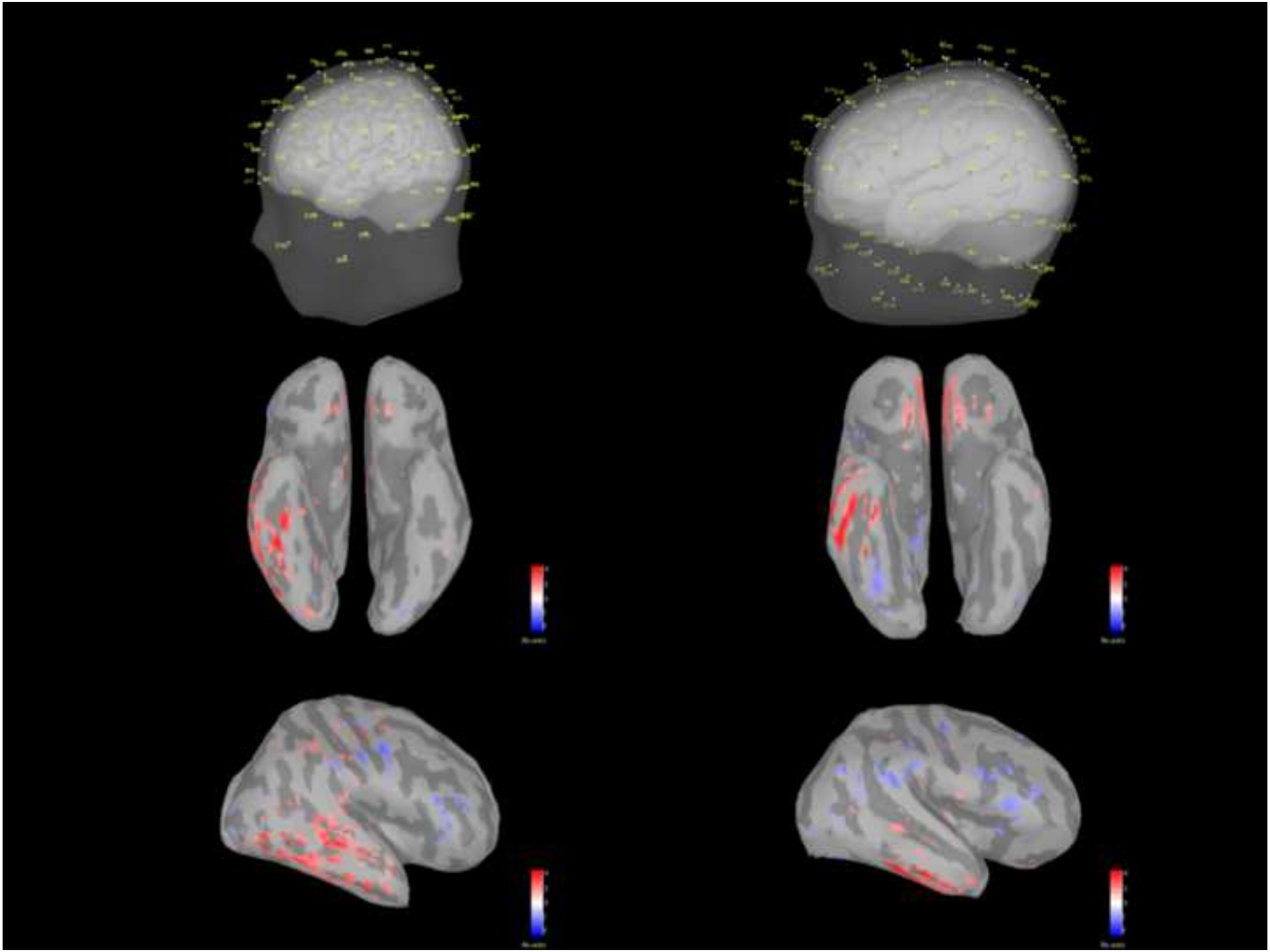

Figure 7 R3
Click here to download high resolution image

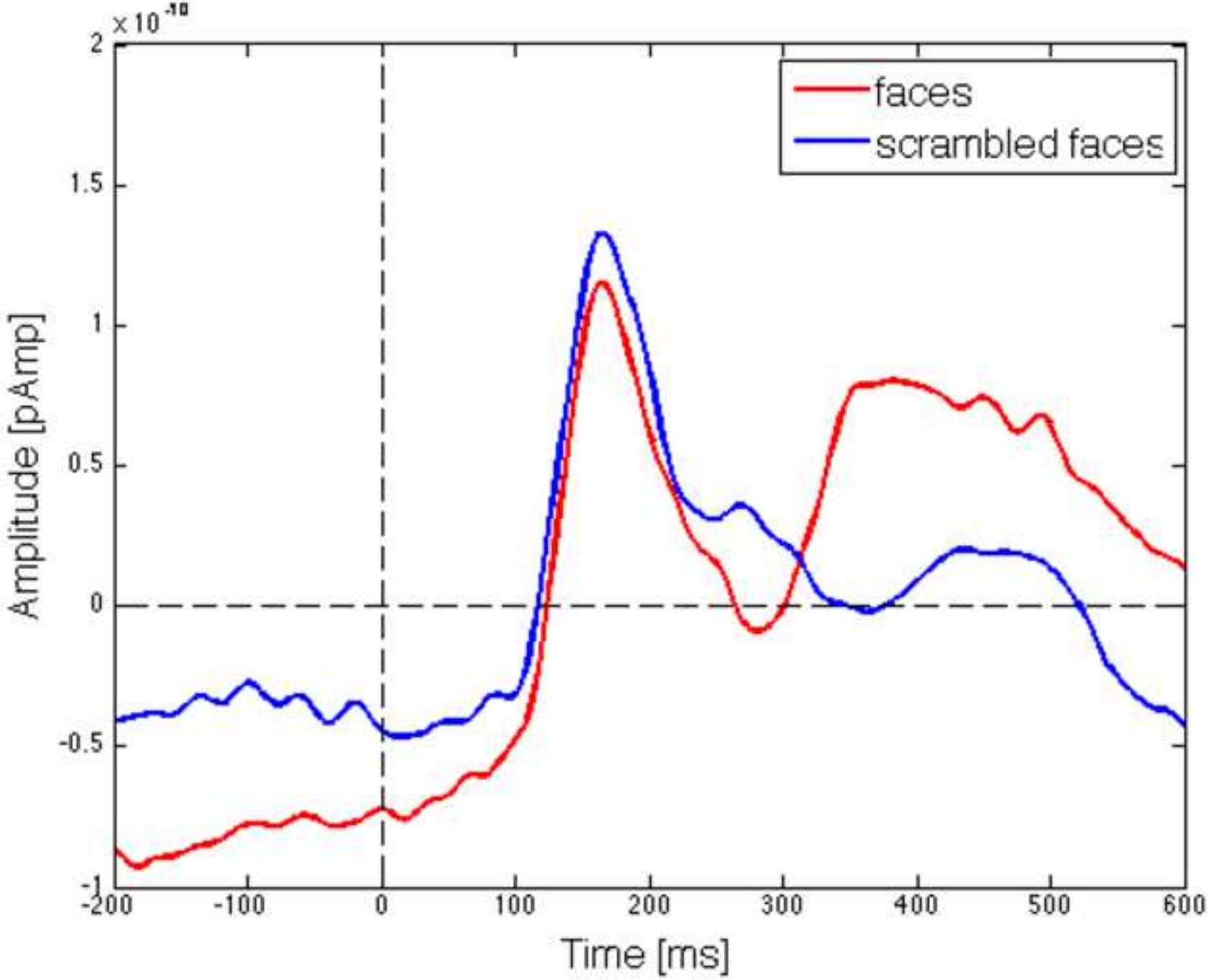

Table
Click here to download Table: Code_File_V2.xlsx

Input for step 1.1

```
input_image = imread('/Users/some_user/images/example.jpeg');
gray_image = rgb2gray(input_image);
saveas(gray_image,'grey_image.tiff')
```

Input for step 1.2

Code Example:

```
%%%%%%%%%%%%%%%%%%%%%%%%%%%%%%%%%%%%%%%%%%%%
% Housekeeping
%%%%%%%%%%%%%%%%%%%%%%%%%%%%%%%%%%%%%%%%%%%%
clc
clear all
close all
InitializePsychSound([0]);
%%%%%%%%%%%%%%%%%%%%%%%%%%%%%%%%%%%%%%%%%%%
% Variables
%%%%%%%%%%%%%%%%%%%%%%%%%%%%%%%%%%%%%%%%%%%%
input_folder = 'C:\Documents and Settings\ERP Lab Users\My
Documents\MATLAB\Faces_Houses\';
netstation = 1;


no_of_trials = 80;
KbName('UnifyKeyNames')


escapeKey = KbName('ESCAPE');
%%%%%%%%%%%%%%%%%%%%%%%%%%%%%%%%%%%%%%%%%%%%
% Loading stimuli
%%%%%%%%%%%%%%%%%%%%%%%%%%%%%%%%%%%%%%%%%%%%
face_directory = strcat('C:\Documents and Settings\ERP Lab Users\My
Documents\MATLAB\Faces_Houses\Faces\');

files = dir(face_directory);
faces  = {files.name};
faces(1:2) = [];

grabbers = dir('/Users/joebathelt/Dropbox/preterm_oddball/grabbers/');
grabbers = {grabbers.name};
grabbers(1:2) = [];

grabber_sounds = dir('/Users/joebathelt/Dropbox/preterm_oddball/sounds/');
grabber_sounds = {grabber_sounds.name};
grabber_sounds(1:2) = [];
```

```
%%%%%%%%%%%%%%%%%%%%%%%%%%%%%%%%%%%%%%%%%%%%%%
% Starting the experiment
%%%%%%%%%%%%%%%%%%%%%%%%%%%%%%%%%%%%%%%%%%%%%%
if netstation == 1;     NetStation('Connect','194.82.245.131','55513')
    NetStation('Synchronize',10)
    NetStation('StartRecording')
end
% Setting up the screen
screenNum=0;

[display.w, display.rect] = Screen('OpenWindow', screenNum, 0);
[wPtr,rect]=Screen('OpenWindow',screenNum);
HideCursor;
black=BlackIndex(wPtr);
Screen('FillRect',wPtr,black);
Screen('TextFont', display.w, 'Arial');
Screen('TextSize', display.w, 32);
Screen('TextStyle',display.w, 0);
for i=1:no_of_trials
FlushEvents
randomizer = randi(2);

attention_grabber =
imread(strcat(input_folder,'grabbers/',cell2mat(grabbers(randi(length(grabbers))))));
    [sounds,fs,nbits] =
wavread(strcat(input_folder,'sounds/',cell2mat(grabber_sounds(randi(length(grabbers))))));
audio_handle = PsychPortAudio('Open', [], [], 0, fs, length(sounds(1,:)));
sounds = sounds';
PsychPortAudio('FillBuffer', audio_handle, sounds);

stimulus = strcat(face_directory,faces(randi(length(faces))));
stimulus = imread(cell2mat(stimulus));

if randomizer == 2;
stimulus = stimulus(randperm(length(stimulus(:,1))),randperm(length(stimulus(1,:))));
end

stim=Screen('MakeTexture', wPtr, double(stimulus)); % stimulus

%%%%%%%%%%%%%%%%%%%%%%%%%%%%%%%%%%%%%%%%%%%%%%
% Trial
%%%%%%%%%%%%%%%%%%%%%%%%%%%%%%%%%%%%%%%%%%%%%%

if i == 1;
```

```
[nx, ny, box] = DrawFormattedText(wPtr, 'Press any key to start', 'center', 'center',[255 255 255]);

Screen('FrameRect', wPtr, 0, box);
[VBLTimestamp StimulusOnsetTim] = Screen('Flip', wPtr);
KbWait([], 2);
[nx, ny, box] = DrawFormattedText(display.w, ' ', 'center', 'center',255); % blank screen
Screen('FrameRect', display.w, 0, box);
[VBLTimestamp StimulusOnsetTim] = Screen('Flip', wPtr);
end

% Fixation Cross
[nx, ny, bbox] = DrawFormattedText(wPtr, '+', 'center', 'center',255);
Screen('FrameRect', display.w, 0, bbox);
[VBLTimestamp StimulusOnsetTim] = Screen('Flip', wPtr);

if netstation == 1;
NetStation('Event','fix+',StimulusOnsetTim) end

WaitSecs(0.15+rand*0.5)


% Stimulus
Screen('DrawTexture', wPtr, stim);
[VBLTimestamp StimulusOnsetTim] = Screen(wPtr, 'Flip');
if netstation == 1;
if randomizer == 1;
NetStation('Event','face',StimulusOnsetTim)
elseif randomizer == 2;
NetStation('Event','scra',StimulusOnsetTim)
end
end
WaitSecs(0.5)

[nx, ny, box] = DrawFormattedText(wPtr, ' ', 'center', 'center',255); % blank screen
Screen('FrameRect', wPtr, 0, box);
[VBLTimestamp StimulusOnsetTim] = Screen('Flip',wPtr);

WaitSecs(1+rand(1))

% Attention grabber
Screen('DrawTexture', wPtr, grabber);
sounds = PsychPortAudio('Start', audio_handle,15, 0, 1);
[VBLTimestamp StimulusOnsetTim] = Screen('Flip',wPtr);
if netstation == 1;
```

```
NetStation('Event','grbr',StimulusOnsetTim)
end

KbWait([], 2);

PsychPortAudio('Stop',audio_handle);
Screen('FrameRect', display.w, 0, box);
[VBLTimestamp StimulusOnsetTim] = Screen('Flip',wPtr);

[keyIsDown, timeSecs, keyCode ] = KbCheck; if keyIsDown
if keyCode(escapeKey)
disp('ESC')
sca
NetStation('StopRecording')
return
end
end
end

Screen('CloseAll');
if netstation == 1;
NetStation('StopRecording')
end
```

Input for step 3.1.1

```
OUTEEG = pop_eegfilt(INEEG,0.1,[]);
```

Input for step 3.1.2

```
OUTEEG = pop_eegfilt(INEEG,[],30);
```

Input for step 3.1.3

```
OUTEEG = pop_epoch(INEEG,‘event’,{‘face’,‘scra’},[-0.2 0.6]);

OUTEEG = pop_rmbase(EEG,[-0.2 0]);
```

Input for step 3.1.4

```
function [EEG] = threshold_rejection(EEG,threshold)
```

```
for j=1:2
for i = 1:length(EEG.data(1,1,:))
data = EEG.data(:,:,i);
data = data - mean(data,2);
maxima = max(abs(data'))';
bad_channels = maxima>threshold;
channel_rejection(:,i) = bad_channels;

if sum(bad_channels) > 0.2*128
      epoch_rejection(i) = 1;
   else
      epoch_rejection(i) = 0;
   end

end
if j==1;
   EEG = pop_select(EEG,'trial',find(epoch_rejection==0))

else
   bad_channels = mean(channel_rejection,2)>0.2;
EEG = pop_interp(EEG,find(bad_channels == 1),'spherical');
end
end
```

Input for step 3.1.5

```
EEG = pop_reref(EEG,[]);
```

Input for step 3.2.1

```
channels = {'E84', 'E89', 'E90', 'E91', 'E94','E95','E96'}; % right N170

EEG = pop_select( EEG,'channel',channels);
Virtual_channel = mean(EEG.data,1);
```

Input for step 3.3.2

```
N170_peak = max(abs((averaged_ERPs(0.13*srate+0.2*srate:0.2*srate+0.2*srate),[],2));
N170_peaklatency = 1000*(find(averaged_ERP(0.13*srate+0.2*srate:0.2*srate+0.2*srate) ==
N170_peak) + 0.2*EEG.srate + 0.13 EEG.srate)./EEG.srate
N170_mean = mean(averaged_ERPs:,0.13*srate+0.2*srate:0.2*srate+0.2*srate),[],2);
```

Description

% Reading the image
% Transferring from RGB to grey scale
% Save new image

Description

% clearing variables from workspace

% setting audio drivers to low latency mode

% defining the working directory

% this toggles communication with NetStation EEG recording software
% defining the number of trials
% unifying keyboard names for easy portability between Unix and PC versions
% defining a variable for a escape key presses

% supplying the folder with stimuli pictures

% generating a list with all picture stimuli

% synchronisation with the recording software
% synchronisation within 10ms of accuracy
% starts the recording

% identification number of presentation screen
% defining a window for stimulus presentation

% hiding the mouse cursor

% setting the background to black
% defining font and font size for text display

% randomly selecting an attention grabber picture

% randomly selecting an attention grabber sound

% setting up sound presentation

% this randomises the presentation of faces and scrambled faces

% loading the stimulus that was randomly selected from the list of stimuli

% scrambling the stimulus matrix, if the trial is a scrambled trial

% preparing the stimulus for presentation

% this section is only relevant to the first trial

% for the first trial, the text “Press any key to start” is presented until a key is pressed

% preparing a white plus sign in the centre of the screen as the fixation cross

% presenting the fixation cross

% sending a trigger with the time stamp of the fixation cross presentation and the code “fix” to the EEG recording software

% limiting presentation time of the fixation cross to a random duration between 0.15 and 0.2s

% presenting the face or scrambled face stimulus

% sending trigger with time stamp and code ‘face’ or ‘scra’ face to EEG recording software

% limit stimulus duration to 500ms
% presenting a blank screen

% inter-trial interval with a random duration between 1 and 2s

% present the attention grabber with sound

% send the time stamp and code for the attention grabber to the EEG recording software

% present the attention grabber and sound until a key on the keyboard is pressed

% abort the experiment, if the escape key was pressed

% close the experiment and stop the EEG recording at the end of the experiment

Description

% OUTEEG = EEG data after filtering, i.e. function output
% INEEG = EEG data before filtering, i.e. function input
% 0.1: high-pass cut-off frequency
% []: low-pass cut-off, undefined because a high-pass filter is desired

Description

% []: high-pass cut-off, undefined because a low-pass filter is desired
% 30: low-pass cut-off frequency

Description

% Epoching
% 'event',{'face','scra'}: the function is told to use the trigger events 'face' and 'scra' as the time-locking markers. These triggers were defined in the experiment script to mark the onset of face and scrambled face stimulus presentation onset
% [-0.2 0.6] = time window for the ERP from 0.2s before the time-locking event to 0.6s
% Removing the baseline
% [-0.2 0]: baseline time window, i.e. 0.2s before the time-locking event to the time-locking event

Description

% function definition, the function requires an EEG dataset structure and a threshold in μV

% this loops goes through all epochs in a given EEG data set

% subtracting the mean activity to avoid the influence of amplitude shifts
% identifying the maximum absolute activity in all channels

% If more than 20% of channels are above the threshold, the epoch is marked for rejection

% selecting only the epochs that are not marked as bad

% mark channels that are bad in more than 20% of epochs after epoch rejection for channel rejection

% apply spherical interpolation to bad channels

Description

% calculates the average reference

Description

% Occipito-temporal channels of the right hemisphere % for N170 responses using the channel labels for the % 128 channels Geodesic Hydrocel Sensor Net
% Selecting the channels
% Combining the individual channels to a virtual channel

Description

% Maximum amplitude within a latency window for each participant in µV

% Peak latency in ms

% Mean amplitude in µV

*Excel Spreadsheet- Table of Materials/Equipment
Click here to download Excel Spreadsheet- Table of Materials/Equipment: JoVE_materials.xlsx

Material

High-density EEG sensor net (128 or 256 channels)
EEG high impendance amplifier
Data Acquisition Computer
Stimulus Presentation Computer
Stimulus Presentation Software
EEG recording software
EEG analysis software

MRI processing software

References

Delorme, A., & Makeig, S. (2004). EEGLAB: an open source toolbox for ana
Sylvain, B., John, C., Dimitrios, P., & Richard, M. (2011). Brainstorm: A Use
Fischl, B., Van Der Kouwe, A., Destrieux, C., Halgren, E., Ségonne, F., Salat
Gramfort, A., Papadopoulo, T., Olivi, E., & Clerc, M. (2010). OpenMEEG: o
Brainard, D. H. (1997). The psychophysics toolbox. Spatial vision.

Make/Model used
HydroCel Geodesic Sensor Net 128
NetAmps 200
PowerMac G4
Optiplex 745
Matlab R2012b with PsychToolBox
NetStation 4.5.1
Matlab R2012b
EEGLAB
BrainStorm
FreeSurfer
OpenMEEG

alysis of single-trial EEG dynamics including independent component a
er-Friendly Application for MEG/EEG Analysis. Computational Intelliger
, D. H., et al. (2004). Automatically parcellating the human cerebral co
pensource software for quasistatic bioelectromagnetics. BioMedical E

Manufacturer
Electrical Geodesic Inc., Oregon, US
Electrical Geodesic Inc., Oregon, US
Apple Inc, California, US
Dell Computers Inc., Texas, US
Brainard et al. 1997
Electrical Geodesic Inc., Oregon, US
The Mathworks Inc.,
Delorme et al. 2004
Sylvain et al. 2001
Fischl et al. 2004
Gramfort et al. 2010

analysis. Journal of Neuroscience Methods, 134(1), 9–21.
nce and Neuroscience, 2011, 1–13.
rtex. Cerebral Cortex, 14(1), 11–22.
ngineering OnLine, 9(1), 45. doi:10.1186/1475-925X-9-45

17 Sellers Street
Cambridge, MA 02139
tel. +1.617.945.9051
www.JoVE.com

ARTICLE AND VIDEO LICENSE AGREEMENT - UK

Title of Article: Cortical source analysis of high-density EEG recordings in children

Author(s): J. Bathelt, H. O'Reilly, M. de Haan

Item 1 (check one box): The Author elects to have the Materials be made available (as described at http://www.jove.com/publish) via: ☒ Standard Access ☐ Open Access

Item 2 (check one box):

☒ The Author is NOT a United States government employee.

☐ The Author is a United States government employee and the Materials were prepared in the course of his or her duties as a United States government employee.

☐ The Author is a United States government employee but the Materials were NOT prepared in the course of his or her duties as a United States government employee.

ARTICLE AND VIDEO LICENSE AGREEMENT

1. Defined Terms. As used in this Article and Video License Agreement, the following terms shall have the following meanings: "**Agreement**" means this Article and Video License Agreement; "**Article**" means the article specified on the last page of this Agreement, including any associated materials such as texts, figures, tables, artwork, abstracts, or summaries contained therein; "**Author**" means the author who is a signatory to this Agreement; "**Collective Work**" means a work, such as a periodical issue, anthology or encyclopedia, in which the Materials in their entirety in unmodified form, along with a number of other contributions, constituting separate and independent works in themselves, are assembled into a collective whole; "**CRC License**" means the Creative Commons Attribution 3.0 Agreement, the terms and conditions of which can be found at: http://creativecommons.org/licenses/by/3.0/us/legalcode; "**Derivative Work**" means a work based upon the Materials or upon the Materials and other pre-existing works, such as a translation, musical arrangement, dramatization, fictionalization, motion picture version, sound recording, art reproduction, abridgment, condensation, or any other form in which the Materials may be recast, transformed, or adapted; "**Institution**" means the institution, listed on the last page of this Agreement, by which the Author was employed at the time of the creation of the Materials; "**JoVE**" means MyJove Corporation, a Massachusetts corporation and the publisher of *The Journal of Visualized Experiments;*

"**Materials**" means the Article and / or the Video; "**Parties**" means the Author and JoVE; "**Video**" means any video(s) made by the Author, alone or in conjunction with any other parties, or by JoVE or its affiliates or agents, individually or in collaboration with the Author or any other parties, incorporating all or any portion of the Article, and in which the Author may or may not appear.

2. Background. The Author, who is the author of the Article, in order to ensure the dissemination and protection of the Article, desires to have the JoVE publish the Article and create and transmit videos based on the Article. In furtherance of such goals, the Parties desire to memorialize in this Agreement the respective rights of each Party in and to the Article and the Video.

3. Grant of Rights in Article. In consideration of JoVE agreeing to publish the Article, the Author hereby grants to JoVE, subject to **Sections 4** and **7** below, the exclusive, royalty-free, perpetual (for the full term of copyright in the Article, including any extensions thereto) license (a) to publish, reproduce, distribute, display and store the Article in all forms, formats and media whether now known or hereafter developed (including without limitation in print, digital and electronic form) throughout the world, (b) to translate the Article into other languages, create adaptations, summaries or extracts of the Article or other Derivative Works (including, without limitation, the Video) or Collective Works based on all or any portion of the Article and exercise all of the rights set forth in (a) above in such translations, adaptations, summaries, extracts, Derivative Works or Collective Works and

(c) to license others to do any or all of the above. The foregoing rights may be exercised in all media and formats, whether now known or hereafter devised, and include the right to make such modifications as are technically necessary to exercise the rights in other media and formats. If the "Open Access" box has been checked in **Item 1** above, JoVE and the Author hereby grant to the public all such rights in the Article as provided in, but subject to all limitations and requirements set forth in, the CRC License.

4. Retention of Rights in Article. Notwithstanding the exclusive license granted to JoVE in **Section 3** above, the

Author shall, with respect to the Article, retain the non-exclusive right to use all or part of the Article for the non-commercial purpose of giving lectures, presentations or teaching classes, and to post a copy of the Article on the Institution's website or the Author's personal website, in each case provided that a link to the Article on the JoVE website is provided and notice of JoVE's copyright in the Article is included. All non-copyright intellectual property rights in and to the Article, such as patent rights, shall remain with the Author.

5. Grant of Rights in Video – Standard Access. This **Section 5** applies if the "Standard Access" box has been checked in **Item 1** above or if no box has been checked in **Item 1** above. In consideration of JoVE agreeing to produce, display or otherwise assist with the Video, the Author hereby acknowledges and agrees that, Subject to **Section 7** below, JoVE is and shall be the sole and exclusive owner of all rights of any nature, including, without limitation, all copyrights, in and to the Video. To the extent that, by law, the Author is deemed, now or at any time in the future, to have any rights of any nature in or to the Video, the Author hereby disclaims all such rights and transfers all such rights to JoVE.

6. Grant of Rights in Video – Open Access. This **Section 6** applies only if the "Open Access" box has been checked in **Item 1** above. In consideration of JoVE agreeing to produce, display or otherwise assist with the Video, the Author hereby grants to JoVE, subject to **Section 7** below, the exclusive, royalty-free, perpetual (for the full term of copyright in the Article, including any extensions thereto) license (a) to publish, reproduce, distribute, display and store the Video in all forms, formats and media whether now known or hereafter developed (including without limitation in print, digital and electronic form) throughout the world, (b) to translate the Video into other languages, create adaptations, summaries or extracts of the Video or other Derivative Works or Collective Works based on all or any portion of the Video and exercise all of the rights set forth in (a) above in such translations, adaptations, summaries, extracts, Derivative Works or Collective Works and (c) to license others to do any or all of the above. The foregoing rights may be exercised in all media and formats, whether now known or hereafter devised, and include the right to make such modifications as are technically necessary to exercise the rights in other media and formats.

7. Government Employees. If the Author is a United States government employee and the Article was prepared in the course of his or her duties as a United States government employee, as indicated in **Item 2** above, and any of the licenses or grants granted by the Author hereunder exceed the scope of the 17 U.S.C. 403, then the rights granted hereunder shall be limited to the maximum rights permitted under such statute. In such case, all provisions contained herein that are not in conflict with such statute shall remain in full force and effect, and all provisions contained herein that do so conflict shall be deemed to be amended so as to provide to JoVE the maximum rights permissible within such statute.

8. Likeness, Privacy, Personality. The Author hereby grants JoVE the right to use the Author's name, voice, likeness, picture, photograph, image, biography and performance in any way, commercial or otherwise, in connection with the Materials and the sale, promotion and distribution thereof. The Author hereby waives any and all rights he or she may have, relating to his or her appearance in the Video or otherwise relating to the Materials, under all applicable privacy, likeness, personality or similar laws.

9. Author Warranties. The Author represents and warrants that the Article is original, that it has not been published, that the copyright interest is owned by the Author (or, if more than one author is listed at the beginning of this Agreement, by such authors collectively) and has not been assigned, licensed, or otherwise transferred to any other party. The Author represents and warrants that the author(s) listed at the top of this Agreement are the only authors of the Materials. If more than one author is listed at the top of this Agreement and if any such author has not entered into a separate Article and Video License Agreement with JoVE relating to the Materials, the Author represents and warrants that the Author has been authorized by each of the other such authors to execute this Agreement on his or her behalf and to bind him or her with respect to the terms of this Agreement as if each of them had been a party hereto as an Author. The Author warrants that the use, reproduction, distribution, public or private performance or display, and/or modification of all or any portion of the Materials does not and will not violate, infringe and/or misappropriate the patent, trademark, intellectual property or other rights of any third party. The Author represents and warrants that it has and will continue to comply with all government, institutional and other regulations, including, without limitation all institutional, laboratory, hospital, ethical, human and animal treatment, privacy, and all other rules, regulations, laws, procedures or guidelines, applicable to the Materials, and that all research involving human and animal subjects has been approved by the Author's relevant institutional review board.

10. JoVE Discretion. If the Author requests the assistance of JoVE in producing the Video in the Author's facility, the Author shall ensure that the presence of JoVE employees, agents or independent contractors is in accordance with the relevant regulations of the Author's institution. If more than one author is listed at the beginning of this Agreement, JoVE may, in its sole discretion, elect not take any action with respect to the Article until such time as it has received complete, executed Article and Video License Agreements from each such author. JoVE reserves the right, in its absolute and sole discretion and without giving any reason therefore, to accept or decline any work submitted to JoVE. JoVE and its employees, agents and independent contractors shall have full, unfettered access to the facilities of the Author or of the Author's institution as necessary to make the Video, whether actually published or not. JoVE has sole discretion as to the method of making and publishing the Materials, including,

17 Sellers Street
Cambridge, MA 02139
tel. +1.617.945.9051
www.JoVE.com

ARTICLE AND VIDEO LICENSE AGREEMENT

without limitation, to all decisions regarding editing, lighting, filming, timing of publication, if any, length, quality, content and the like.

11. Indemnification. The Author agrees to indemnify JoVE and/or its successors and assigns from and against any and all claims, costs, and expenses, including attorney's fees, arising out of any breach of any warranty or other representations contained herein. The Author further agrees to indemnify and hold harmless JoVE from and against any and all claims, costs, and expenses, including attorney's fees, resulting from the breach by the Author of any representation or warranty contained herein or from allegations or instances of violation of intellectual property rights, damage to the Author's or the Author's institution's facilities, fraud, libel, defamation, research, equipment, experiments, property damage, personal injury, violations of institutional, laboratory, hospital, ethical, human and animal treatment, privacy or other rules, regulations, laws, procedures or guidelines, liabilities and other losses or damages related in any way to the submission of work to JoVE, making of videos by JoVE, or publication in *JoVE* or elsewhere by JoVE. The Author shall be responsible for, and shall hold JoVE harmless from, damages caused by lack of sterilization, lack of cleanliness or by contamination due to the making of a video by JoVE its employees, agents or independent contractors. All sterilization, cleanliness or decontamination procedures shall be solely the responsibility of the Author and shall be undertaken at the Author's expense. All indemnifications provided herein shall include JoVE's attorney's fees and costs related to said losses or damages. Such indemnification and holding harmless shall include such losses or damages incurred by, or in connection with, acts or omissions of JoVE, its employees, agents or independent contractors.

12. Fees. To cover the cost incurred for publication, JoVE must receive payment before production and publication the Materials. Payment is due in 21 days of invoice. Should the Materials not be published due to an editorial or production decision, these funds will be returned to the Author. Withdrawal by the Author of any submitted Materials after final peer review approval will result in a US$1,200 fee to cover pre-production expenses incurred by JoVE. If payment is not received by the completion of filming, production and publication of the Materials will be suspended until payment is received.

13. Transfer, Governing Law. This Agreement may be assigned by JoVE and shall inure to the benefits of any of JoVE's successors and assignees. This Agreement shall be governed and construed by the internal laws of the Commonwealth of Massachusetts without giving effect to any conflict of law provision thereunder. This Agreement may be executed in counterparts, each of which shall be deemed an original, but all of which together shall be deemed to me one and the same agreement. A signed copy of this Agreement delivered by facsimile, e-mail or other means of electronic transmission shall be deemed to have the same legal effect as delivery of an original signed copy of this Agreement.

A signed copy of this document must be sent with all new submissions. Only one Agreement required per submission.

AUTHOR:

Name: Johannes Bathelt

Department: Institute of Child Health

Institution: University College London (UCL)

Article Title: Cortical source analysis of high-density fTCD recordings in children

Signature: J. Bathelt Date: 9/10/2013

Please submit a signed and dated copy of this license by one of the following three methods:

1) Upload a scanned copy as a PDF to the *JoVE* submission site upon manuscript submission (preferred);
2) Fax the document to +1.866.381.2236; or
3) Mail the document to *JoVE* / Attn: *JoVE* Editorial / 17 Sellers St / Cambridge, MA 02139

For questions, please email editorial@jove.com or call +1.617.945.9051.

MS # (internal use):

JoVE Revision: Response to Reviewers' comments

1) some of the paragraphs have several topics of information (e.g., 83 to 96) that might be separated into separate paragraphs. For example, perhaps all the information about structural and fMRI could be in one paragraph (description, strengths, weaknesses), one with EEG, and one with source analysis. Following this, one could then make comparative judgements better.

The structure of the article and the content of the section was revised

2) Second, perhaps a slight bit more could be said about the models used for source analysis. The procedure introduces the BEM method, and MNE; but little information is given about what these are, why alternative models (FEM; LORETA; sLORETA) might be useful. The paper also states that BEM methods only show activity on the cortical surface. The BEM method describes the head model and forward/inverse lead-field matrices for the biophysical properties of the head. However, the sources for the BEM model need to be specified and can include any elements inside the inner compartment (e.g. gray matter voxels inside the inner comparement).

A section with a short overview of the most commonly used models and inverse solution algorithms was added to the introduction. References are provided for reviews and technical notes that discuss the topic in more detail.

3) Third, one missing component in the introduction is the application of these methods to children. Whereas there is sufficient information to show

the motivation for using EEG rather than fMRI, one wonders if there are special considerations for children with the source analysis methods (conductivity of elements different? Head size effects? Electrode placement?).

a section was added to the discussion that addresses the limitation of the technique and applicability to children

4) Is there a need for exact sensor positions on the head?

Standard electrode positions can be used for source reconstruction when the fit is adjusted using age-appropriate or individual anatomical scans (see step 3.5.5). However, we observed in our lab that the fit of electrode nets is quite variable. For instance, the participant's head circumference may be at the lower or upper cut-off for a particular net size, which leads to a tight or loose fit. Digitisations systems help to quantify this variability and build it into the model. We are not aware of any study that compared source solutions using adjusted standard positions and positions based on digitisation, but agree that a study like this would be a very useful addition to the literature.

5) The paper mentions spatial digitization systems, perhaps should give examples. (e.g., Polhemus; EGI GPS system; average age-appropriate electrode maps).

A note with reference to different digitisation systems was added to step 2.5 following the reviewer's suggestion.

5) In 3.2.8 the paper says to select a channel position file from the mfr or EEGLab www site. However, there is no information given about how this will

fit on the MRI scan that is used to do the BEM model. In source analysis the positions of the electrodes must be specified in the source model (lead-field matrix). How is this done with mfr / EEGLab locations? Do you need locations specified for the exact MRI that is being used? (either individual, or age-appropriate avg). incidentally, mfrs and EEGLab have adult head position electrode maps. What about child maps?

All processing steps up to section 3.4 describe transformations on the channel level. The independent component analysis algorithm that is used for pre-processing does not take anatomical information into consideration. Instead, differences in channel statistics are used to separate the data. Step 3.5.5 described how channel location information is aligned with the MRI. Briefly, the nation, and left and right periauricular point need to be identified on the anatomical scan. The remaining channels are warped to the skull surface accordingly. Because of space constraints, we refer to the website of the analysis software developers that covers this topic in some detail.

6) 2.1 to 2.9 Perhaps refer to the EGI instructions for net preparation and application.

A reference to the EGI instructions was added. We think that the net application and general testing procedures are particularly well suited for the video format of the Journal of Visualized Experiments, because many of the testing practices for young participants are hard to convey in writing.

7) Perhaps describe the BEM (and other models) in the introduction. Also, perhaps it should be mentioned that most of the available source analysis tools do BEM (BESA, Curry, EMSE, EEGLab). Also, perhaps lay out the case why BEM models are sufficient, when some literature suggest some improvement with FEM methods. Also, CURRY, EMSE, and BESA, allow the calculation of the head model via GUI-driven segmenting methods. They do this for individual participants, or for average MRIs, and then analyses are based on the head model for that MRI rather than for an adult average head model.

A section discussing different head models was added to the introduction.

8) 3.4 A brief note is stated about using age-appropriate MRI templates, or individual MRIs. I believe there is no literature that compares the efficacy of individual MRIs with children vs age-appropriate MRIs; or even age-appropriate vs adult MRIs. I agree with the authors about the need for individual/age-appropriate MRIs, but perhaps this issue should be addressed in the introduction and/or discussion. A paper comparing the age-appropriate with adult-head models, vis-à-vis cortical source analysis, would be a useful addition to the literature.

A study by Brodbeck and colleagues (Brodbeck et al., 2011) compared sensitivity and specificity for detecting sources of focal epileptic activity in a sample of 152 children using individual and template standard head models. They report high sensitivity and specificity when individual MRI are used for the source models (84%,88%) for source reconstruction of hdEEG and lower values when template models are

used (76%,55%). We are not aware of any study that compares individual, age-appropriate, and adult template head models. A possible reason for this gap in the literature is that average MRIs for developmental populations only become available relatively recently (see Sanchez et al. 2012). Using BEMs, it is reasonable to assume that the accuracy of age-appropriate templates is closer to head models based on individual MRIs than adult templates. We agree that a comparative study as suggested by the reviewer would be a very useful addition to the literature.

Brodbeck, V., Spinelli, L., Lascano, A. M., Wissmeier, M., Vargas, M. I., Vulliemoz, S., et al. (2011). Electroencephalographic source imaging: A prospective study of 152 operated epileptic patients. Brain, 134(10), 2887–2897. doi:10.1093/brain/awr243

Sanchez, C. E., Richards, J. E., & Almli, C. R. (2012). Age-specific MRI templates for pediatric neuroimaging. Developmental Neuropsychology, 37(5), 379–399. doi:10.1080/87565641.2012.688900

Reviewer #2:

Minor Concerns:

Introduction:

1) P4, Lines 133-135: Please explain this sentence (provide an example).

The section was rephrased and expanded

2) The authors should introduce an overview on some of the currently and more used available source localization algorithms (see Michel et al., 2004),

with an empirical example for each: in terms of the most common application of each specific method.

An overview of the most commonly used inverse solution algorithms was added to the introduction.

Analysis:

3) I believe that could it be better say that ICA isn't a mandatory step before source localization analysis: If the data collected are enough clean it is possible avoiding this procedure, how it has been done recently (see Berchio et al. 2013).

An introductory note was added to section 3.2 to clarify that pre-processing with ICA is optional and maybe skipped or replaced with other approaches.

4) Are there any bibliographic references that can sustain these % thresholds?

The percentage thresholds are ball-park figures that were adjusted from processing recommendations for adults to account for the higher amount of artefact in child data. We clarified that researchers may adjust these thresholds for their data.

Bibliographic references for percentage thresholds cannot be supplied, because the exact procedure for data preprocessing is not usually described in ERP papers.

5) This sentence needs to be clarified. The idea that as a rule 'the necessary number of repetitions should be doubled compared to adult studies', it is partially in contradiction to the view that is difficult make EEG experiments

with children.The Authors should suggest more convincing strategies: for example, increase the sample, planning easy task….

The paragraph was revised and extended

6) An important message of the present work it is that in children 'the accuracy of EEG source analysis with standard head models is limited'. It would be useful to include an additional figure: a standard MNI template, with the same contrast analysis (faces vs scrambled faces). The Authors should add some comments in the discussion section and describe any differences in the cortical source responses.

A figure showing the difference between an adult head model and an age appropriated head model for a recording of a 6 year old was added.

Reviewer #3:

1) The Introduction meanders and is repetitive.

The discussion introduction was revised

2) What is the link between Figure 2 at L451 and Figure 4 at L516? Did anyone proofread this?

The figure numbering and references in the text were revised to accommodate the added figures

3) The first para in the Discussion belongs only in the Intro - it's repetitive here.

The discussion was revised according to the reviewers' comments

4) The second sentence in the Short Abstract doesn't make sense.

Line 96: "distant to"?

Line 98:"to take advantages".

Line 166/7: repeat of "for the purposes".

The sentences were changed

5) The EEG reference is not specified - how to replicate?

A note about the reference channel used for recording was added to step 3.1.5

6) Line 244: "Calculate the average reference by...". No, this should be "Re-reference to the average reference by....".

The wording of step 3.1.5 was changed following the reviewer's comment

7) Line 281: I have never seen published data which combines channels as suggested.

The channel selection for channel-level analysis was based on commonly used channels in studies investigating N170 responses to emotional facial expressions {Sherbondy:2008fo}. The exact selection of channels varies between EEG systems and also depends on the preferences of the research group.

We use the channel-level analysis of N170 responses only as an example to illustrate that additional information can be obtained by applying source reconstruction.